

## GEOGENIC RADON AS GEOPHYSICAL TRACER OF ACTIVE FAULTS: THE FUCINO PLAIN (CENTRAL ITALY)

G. Ciotoli<sup>1,2</sup>, L. Ruggiero<sup>3</sup>, G.P. Cavinato<sup>1</sup>, L. Modesti<sup>2</sup>, S. Bigi<sup>2</sup>, V. Romano<sup>4</sup>

<sup>1</sup> Institute of Environmental Geology and Geoengineering, National Research Council, Rome, Italy

<sup>2</sup> National Institute of Geophysics and Volcanology, Rome, Italy

<sup>3</sup> Department of Earth Sciences, Rome University Sapienza, Rome, Italy

<sup>4</sup> Dept. of Geology, University of Illinois, Urbana-Champaign, USA

**Introduction.** In geosciences, the analysis of the spatial distribution of radon (<sup>222</sup>Rn) concentrations in the shallow environment provides insights into a range of primary spatial/temporal geochemical/geophysical processes. Among the soil gases, <sup>222</sup>Rn is considered a convenient fault tracer, because of its ability to migrate to long distances from host rocks, as well as the efficiency of detecting it at very low levels. In the scientific literature, many papers are focused on Rn as tracer of hidden faults, and reported Rn anomalies significantly higher than background levels along active faults and associated fracture zones (King *et al.*, 1996; Ciotoli *et al.*, 2007, 2014, 2016; Davidson *et al.*, 2016). Evidences suggest that these anomalies can provide reliable information about the location and the geometry of active faults, and the width of the surrounding fracture zones (also if buried under the sedimentary cover) (Ciotoli *et al.*, 2016, 2007; Seminsky *et al.*, 2014). In this work, new soil gas measurements were carried out at different scales across known and inferred structural discontinuities in the Fucino plain (central Italy) in order to homogenise and densify the sampling reported in Ciotoli *et al.*, 2007. Dataset has been re-interpreted by using new GIS and geospatial analysis techniques and discussed in the light of new seismic data interpretation (Cara *et al.*, 2011). In particular, the correlation between the distribution of radon anomalies and the offsets measured along the San Benedetto-Gioia dei Marsi Fault (SBGMF) are discussed. Furthermore, new hypotheses are proposed regarding the link between radon migration and the process of fault evolution during the progressive linkage mechanism of several fault segments.

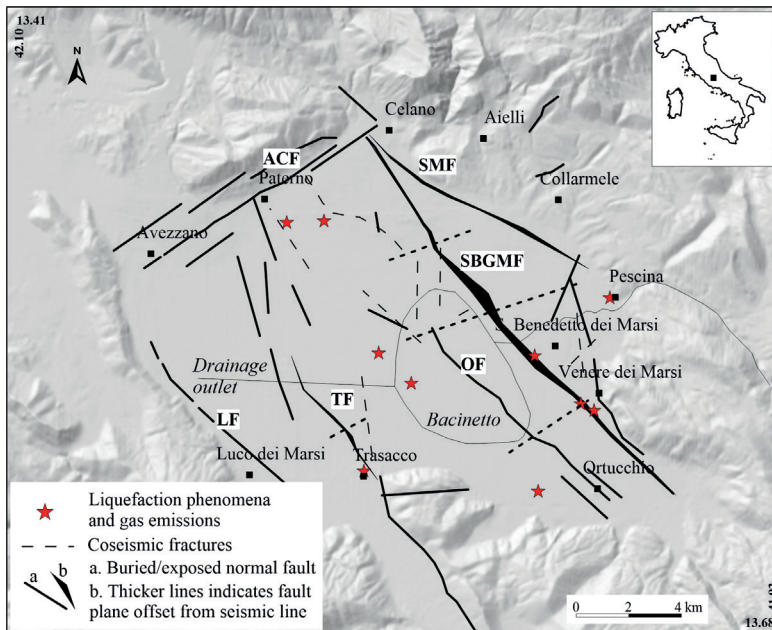


Fig. 1. Main known and buried faults of the Fucino plain. ACF, Avezzano-Celano fault; SMF, Statale Marsicana fault; SBGMF, San Benedetto- Gioia dei Marsi fault; OF, Ortucchio fault, TF, Trasacco fault; LMF, Luco dei Marsi fault. The thickness of the line indicates the fault offset as reported in Cara *et al.*, 2011. Map limits are in WGS84 decimal coordinates.

**The Fucino Plain.** The Fucino plain (Central Italy) is an intramontane basin formed by the extensional tectonics that affected the central-western Apennine range during Late Pliocene (Fig. 1). This tectonic depression is filled by about ~1000 m of Upper Pliocene-Holocene lacustrine and alluvial sediments that unconformably overlie Meso-Cenozoic carbonate substratum (Bosi *et al.*, 1995; Cavinato *et al.*, 2002). The plain is bordered and crossed by a network of buried and/or exposed faults and is characterised by high seismic activity (the plain was struck by the Avezzano earthquake of 13 January 1915). The fault activity is testified by the terraced Middle-Upper Pleistocene alluvial fan and fluvial-lacustrine deposits hanging for hundreds of meters above the present valley floor in the north and north-eastern borders of the basin (Galadini *et al.*, 1997; Cavinato *et al.*, 2002). The main faults recognized in the Fucino basin are: (1) the Avezzano-Celano (ACF-inferred) fault (ENE trending, SE dipping) in the northern sector; (2) the San Benedetto Gioia dei Marsi fault (SBGMF), reactivated during the 1915 Avezzano earthquake, and the Statale Marsicana (SMF) fault in the eastern sector; (3) the Ortucchio fault (OF-inferred) near the center of the basin; and (4) the Trasacco (TF) and Luco dei Marsi (LF) faults (NW trending, SW dipping) in the southwestern sector (Cavinato *et al.*, 2002). The vertical offset across the SBGMF in the Middle and Late Pleistocene very likely exceeds 300 m, providing a slip rate of about 1 mm yr<sup>-1</sup> (Cara *et al.*, 2011). Other seismo-induced geological phenomena (i.e. liquefaction and gas and water emissions) were observed inside the plain (Fig.1).

**Results.** A large number of soil gas samples (more than 1200) were collected in the plain and analysed for different gas species (Rn, CO<sub>2</sub>, He and CH<sub>4</sub>). The soil gas sampling was accomplished by a consolidated procedure reported in Ciotoli *et al.*, 2014. Collected samples are then analyzed by using statistical and geostatistical techniques in order to define the anomaly threshold and construct the soil gas distribution maps. Results, discussed in Ciotoli *et al.*, 2007, highlighted the presence of linear gas anomalies both in correspondence of known and visible faults of the eastern border of the plain (SBGMF), as well as provided clear indication of the presence of buried faults (OF and TF) in correspondence of different cover thickness in the middle of the plain. Geostatistical analysis of radon data provided a correlation between the anisotropic shape and the orientation of radon anomalies, and the different geometry of the faults: broader low anomalies along the TF linked to a wider and low permeability fracture zone in the western sector; highest values and more sharp anomalies along the high permeability fractured zone of the SBGMF in the eastern side of the plain. The re-interpretation of the radon data in the light of the new samplings confirms the presence of anisotropic radon distribution in correspondence of exposed San Benedetto dei Marsi Fault (SBGMF), as well as provided clear indication of the presence of buried Ortucchio Fault (OF) and Trasacco Fault (TF) in the middle of the plain, and Avezzano-Celano Fault (AFC) to the north (Fig. 2).

**Discussion.** The proximity to the fault plane and the bedrock lithology are the main factors controlling the shallow radon emissions. Radon anomalies in the Fucino plain produced a consistent and clear anisotropic distribution that enabled to infer the location of the fault zones (Ciotoli *et al.*, 2007) (Fig. 2). According to literature data, faults are accompanied by Rn anomalies having a simple shape with the maximum values above the main fault and the minimum values on the fault margins (King *et al.*, 1996). However, many studies highlight that Rn anomalies above faults vary in intensities and shapes, as well as radon peak values can assume different spatial position within the fault zone (Ciotoli *et al.*, 2016; Seminsky *et al.*, 2014). The spatial irregular distribution of radon concentrations is predetermined by the more or less complex geometry of the fault zones and their activity, as well as by the volume of fractured rock involved (Annunziatellis *et al.*, 2008).

In general, the evolution of the fault zone is characterized by the stepwise development of a different number of fault planes and of a variable volume of fractured rocks across and along strike. In fact, the process of fault evolution provides a progressive linkage mechanism among many small fault segments, to satisfy a strain localization process. At the early stages, there

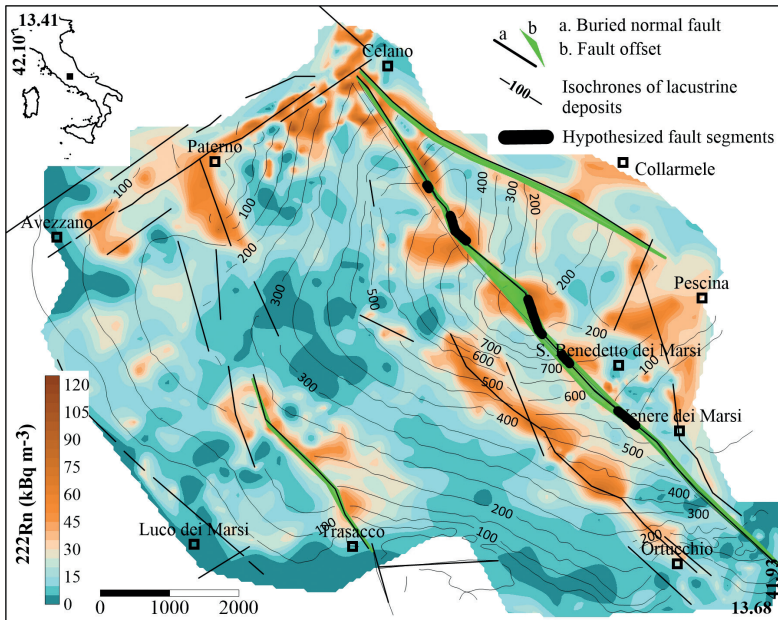


Fig. 2 - Map of the  $^{222}\text{Rn}$  distribution across the Fucino plain. Linear radon anomalies occur along the main faults (buried and exposed) crossing the basin. The map also shows the isochrones (in ms) of the lacustrine deposits reworked by Cavinato *et al.*, 2002. The isochrones map allows the calculation of the fault offsets (green area) along the SBGMF thus suggesting the presence of several faults segments. Highest radon anomalies occur in correspondence of these recognized offsets.

are several slip planes in the active fault zone with different offsets along strike; this suggests that the linkage process is not completed and that the main fault is still formed by a series of segments. On the contrary, at the final stages the zone is largely dominated by a main fault (Fossen, 2010; Peacock *et al.*, 1991). This peculiar evolution of the fault zones will affect the shallow distribution of radon that can show anomalies of various shape and intensity.

Fig. 2 shows the isochrones contour map (continuous lines) expressed in TWT (interval 50 and 100 ms) of the alluvial and lacustrine deposits (Cavinato *et al.*, 2002) overlapping the image color map of radon concentrations in soil gas. As reported in Cara *et al.*, 2011, assuming a  $V_p$  of 2,000 m/s the values of TWT can be interpreted as thickness of sedimentary cover in meters. The cover thickness is then used to estimate the different offsets (light green area in fig. 2) along the main faults. Fig. 2 highlights that radon spot and/or linear anomalies ( $> 30 \text{ kBq m}^{-3}$ ) occur along the strikes of the main faults (buried and exposed) that intersect the basin. We focused the study on the spatial distribution of radon anomalies along the SBMF because it shows the highest offsets.

Assuming that the highest thicknesses measured along the SBGMF correspond to the major offsets, NW-SE profiles of the cover thickness and of the radon concentrations have been elaborated along the fault strike (Fig. 3a). The black segments along the SBGMF represents the fault segments to which corresponds a thickness above the threshold value of 500 ms calculated using a normal probability plot of TWT values. Figure 3a shows a significant coincidence between the peaks of the two variables. In particular, the presence of 4 peaks above the threshold value of 500 ms suggests that the SBGMF shows high and low gas-permeable zone along strike, while low thickness values suggest the presence of fault tips. The thickness decreases along the fault toward SE. Radon profile shows the major peaks in correspondence of the highest offsets, and radon signal also decreases toward SE (Fig. 3a). The presence of high radon values at the starting point of the profile is caused by the intersection of the SBMF with the ACF to the north

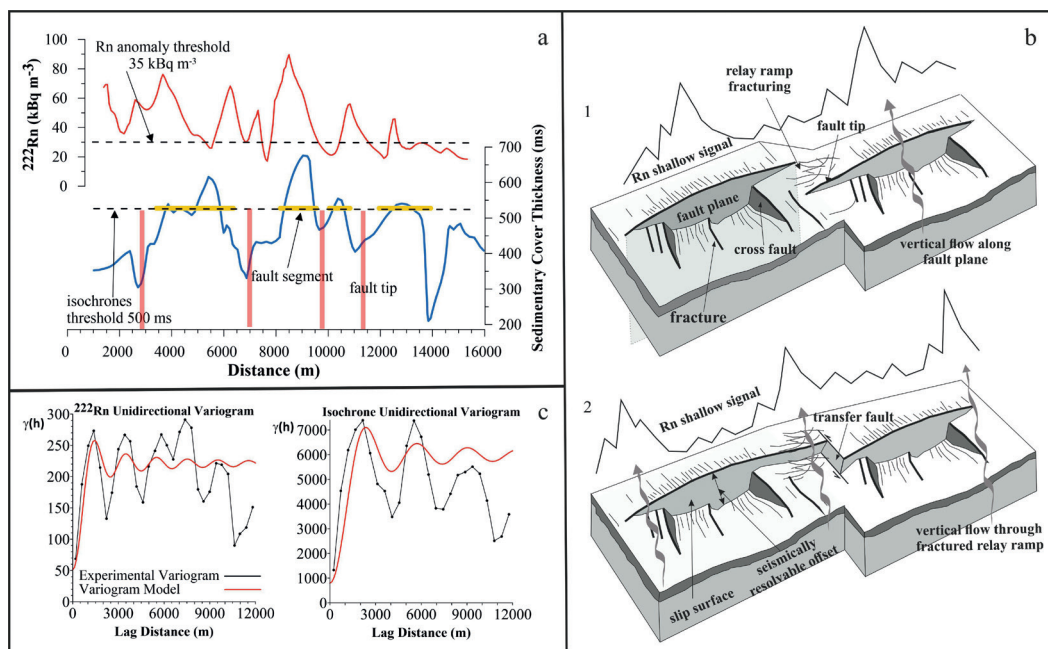


Fig. 3 - Radon and offset profiles along the SBMF (a); shallow radon signal and evolution of the fault zone. 1. Uniform extensive regime generating a series of en-echelon faults in the sedimentary cover, 2. that link up to a non-planar large fault (b); unidirectional variograms calculated for radon concentrations and isochrones values along the SBGMF strike (c).

where the highest radon values were measured (Fig. 2). In correspondence of the first fault segment, radon peaks occur at the fault tips suggesting the presence of fracturing zones, as occur during the linkage process. The other radon peaks occur in correspondence of the highest offset peaks suggesting that in this cases the fault zone is still dominated by fracturing (Fig. 3b).

The spatial variability of Rn and thickness values are also analysed by using unidirectional variograms to verify a spatial cyclicity of the peak values (Fig. 3c). The variograms are modelled with hole effect models that highlight variance peaks with a cyclicity of about 2000 m for radon, and a cyclicity of about 4000 m for the thickness. The cyclicity of the spatial distribution of offsets and radon peaks along the fault strike may confirm the presence of distinct segments of the SBMF with a typical geometry, e.g. relay ramps, suggesting that the linkage process is not completed. The double cyclicity of the cover thickness with respect to the radon values can be interpreted in terms of the evolution of the faults. In fact, as the most fractured area is usually located at the fault tip where relay faults and secondary faults can be developed, this would result in a symmetrical and opposite distribution of the radon anomalies with respect to the progress of the offset (Fossen and Rotevatn , 2016).

**Conclusions.** Radon has received much attention as an effective geophysical tracer of buried faults even in basins with high thickness of unconsolidated cover materials. Linear radon anomalies along the fault strike constitute the main distribution pattern suggesting the extension of the fault domain. However, the intensity of radon anomalies can vary along the fault strike due to permeability and/or porosity changes (i.e., geometry and maturity). In particular, radon distribution appears to be controlled by the highest offsets in the case of early stage of the fault and by presence of highly fractured transfer zones at the tips of the fault segments during the linkage process. This strict link between Rn and fault processes suggests the relation between the stress-strain changes along seismogenic faults and the anomalous signals in geogenic Rn time series. However, results have not been sufficiently conclusive so that a certain dissatisfaction has

taken place in this field of research. The fault characterization with respect to their Rn signature and the understanding of geophysical and geochemical processes at the fault neighboring are necessary prerequisites for their evaluation in terms of seismic prediction. For doing this, it is required: (1) to assess the role of the structural geological factors in the formation of the radon field above the fault zones, (2) to characterise the structural situations determining the pattern of the near fault radon anomalies, and (3) to reveal the levels of radon activity for the faults in the studied region.

## References

- Annunziatellis A., Beaubien S.E., Bigi S., Ciotoli G., Coltella M. and Lombardi S.; 2008: Gas migration along fault systems and through the vadose zone in the Latera caldera (central Italy): Implications for CO<sub>2</sub> geological storage. *International Journal of Greenhouse Gas Control*, **2**, 353-372.
- Bosi, C., Galadini F. and Messina P.; 1995: Stratigrafia plio-pleistocenica della Conca del Fucino. *Quaternario*, **8(1)**, 83-94.
- Cara F., Di Giulio G., Cavinato G.P., Damiani F. and Milana G.; 2011: Seismic characterization and monitoring of Fucino Basin (Central Italy). *Bull. Earthquake Eng.*, **9**, 1961-1985.
- Cavinato, G. P., Carusi C., Dall'Asta M., Miccadei E. and Piacentini T.; 2002: Sedimentary and tectonic evolution of Plio-Pleistocene alluvial lacustrine deposits of Fucino basin (central Italy). *Sediment. Geol.*, **148**, 29–59.
- Ciotoli G., Sciarra A., Ruggiero L., Annunziatellis A. and Bigi S.; 2016: Soil gas geochemical behaviour across buried and exposed faults during the 24 August central Italy earthquake. *Annals of Geophysics*, **59**, Fast Track 5, doi: 10.4401/ag-7242.
- Ciotoli G., Ascione A., Bigi S., Lombardi S. and Mazzoli S.; 2014: Soil gas distribution in the main coseismic surface rupture zone of the 1980, Ms=6.9, Irpinia earthquake (southern Italy). *Journal of Geophysical Research*, **119/3**, 2440–2461, DOI:10.1002/2013JB010508.
- Ciotoli G., Lombardi S. and Annunziatellis A.; 2007: Geostatistical analysis of soil gas data in a high seismic intermontane basin: Fucino Plain, central Italy. *Journal of Geophysical Research*, **112 (B5)**.
- Davidson J.R., Fairley J., Nicol A., Gravley D., and Ring U.; 2016: The origin of radon anomalies along normal faults in an active rift and geothermal area. *Geosphere*; 12 (5), doi:10.1130/GES01321.1.
- Fossen H., Schultz R.A., Rundhovde E., Rotevatn A. and Buckley S.J.; 2010: Fault linkage and graben stepovers in the Canyonlands (Utah) and the North Sea Viking Graben, with implications for hydrocarbon migration and accumulation. *AAPG Bulletin*, **94 (5)**, 597-613, doi:10.1306/10130909088.
- Galadini, F., Galli P., and Giraudi C.; 1997: Geological investigations of Italian earthquakes: New paleoseismological data from the Fucino Plain (central Italy). *J. Geodyn.*, **24(1)-(4)**, 87– 103.
- King C.Y., King B.S., Evans W.C. and Zhang W; 1996: Spatial radon anomalies on active faults in California. *Applied Geochemistry*, **11**, 497-510, doi: 10.1016/0883-2927(96)00003-0.
- Peacock D.C.P. and Sanderson D.J.; 1991: Displacements, segment linkage and relay ramps in normal fault zones. *J. Struct. Geol.*, **13**, 721-733
- Seminsky K.Zh., Bobrov A.A. and Demberel S.; 2014: Variations in Radon Activity in the Crustal Fault Zones: Spatial Characteristics. *Physics of the Solid Earth*, **50 (6)**, 795–813, doi: 10.1134/S1069351314060081.